



THE UNIVERSITY *of* EDINBURGH

## Edinburgh Research Explorer

### Solid–Liquid Equilibria for the CO<sub>2</sub> + R152a and N<sub>2</sub>O + R152a Systems

**Citation for published version:**

Di Nicola, G, Giulianis, G, Polonara, F, Santori, G & Stryjek, R 2007, 'Solid–Liquid Equilibria for the CO<sub>2</sub> + R152a and N<sub>2</sub>O + R152a Systems', *Journal of Chemical and Engineering Data*, vol. 52, no. 6, pp. 2451-2454. <https://doi.org/10.1021/je700384e>

**Digital Object Identifier (DOI):**

[10.1021/je700384e](https://doi.org/10.1021/je700384e)

**Link:**

[Link to publication record in Edinburgh Research Explorer](#)

**Published In:**

Journal of Chemical and Engineering Data

**Publisher Rights Statement:**

This document is the unedited author's version of a Submitted Work that was subsequently accepted for publication in *Journal of Chemical and Engineering Data*, copyright © American Chemical Society after peer review. To access the final edited and published work, see <http://pubs.acs.org/doi/abs/10.1021/je700384e>.

**General rights**

Copyright for the publications made accessible via the Edinburgh Research Explorer is retained by the author(s) and / or other copyright owners and it is a condition of accessing these publications that users recognise and abide by the legal requirements associated with these rights.

**Take down policy**

The University of Edinburgh has made every reasonable effort to ensure that Edinburgh Research Explorer content complies with UK legislation. If you believe that the public display of this file breaches copyright please contact [openaccess@ed.ac.uk](mailto:openaccess@ed.ac.uk) providing details, and we will remove access to the work immediately and investigate your claim.



# SOLID-LIQUID EQUILIBRIA FOR THE CO<sub>2</sub> + R152a, AND N<sub>2</sub>O + R152a SYSTEMS

Giovanni Di Nicola, Giuliano Giuliani, Fabio Polonara, Giulio Santori, and Roman Stryjek\*

*Dipartimento di Energetica, Università Politecnica delle Marche, Ancona, Italy*

*\*Institute of Physical Chemistry, Polish Academy of Sciences, Warsaw, Poland*

## **Abstract**

A recently built experimental set-up was employed for the estimation of the solid-liquid equilibria of alternative refrigerants systems. The behavior of two binaries, i.e. carbon dioxide + 1,1-difluoroethane (CO<sub>2</sub> + R152a) and nitrous oxide + 1,1-difluoroethane (N<sub>2</sub>O + R152a), was measured down to temperatures of 132 K.

The triple points of CO<sub>2</sub> and N<sub>2</sub>O were measured to confirm the reliability of the apparatus. The triple point of R152a was also measured, however the pressure at the triple point for this fluid was too low to accurately measure with current apparatus. All triple point data measured revealed a generally good consistency with the literature.

The results obtained for the mixtures were interpreted by means of the Schröder equation.

## Introduction

The data on SLE are important in refrigerating industry defining the lowest temperature limit at which the refrigerant may circulates in fluid state. In addition, SLE provide theoretical information on the behavior of studied systems at low temperatures in terms of activity coefficients. But, in a fact, the SLE for HFCs refrigerants are extremely scarce in literature.

The  $PVT_x$  of the  $\text{CO}_2 + \text{R152a}$  binary system were recently studied by the same authors with an isochoric apparatus,<sup>1</sup> but no information on the SLE of both title systems are available in the literature. The present study was also undertaken to fill this gap.

Due to expected temperatures of the SLE of the systems formed with  $\text{CO}_2$  and/or  $\text{N}_2\text{O} + \text{HCF}$  refrigerants that usually spans from about 100 up to 217 K (in case of  $\text{CO}_2$  as the mixtures component), SLE measurements generally creates difficulties in the visual observation of the disappearance of the last amount of solid phase. Hence a set-up was specifically built<sup>2</sup> avoiding the need of the visual observation of phase behavior. Recently, the SLE of the  $\text{CO}_2 + \text{N}_2\text{O}$ ,  $\text{CO}_2 + \text{R32}$ , and  $\text{N}_2\text{O} + \text{R32}$  systems<sup>2</sup> and  $\text{CO}_2 + \text{R125}$ , and  $\text{N}_2\text{O} + \text{R125}$  systems<sup>3</sup> were studied. In this paper, the system's behavior was measured down to temperatures of 132 K for two binaries, i.e.  $\text{CO}_2 + \text{R152a}$  and  $\text{N}_2\text{O} + \text{R152a}$ .

## Description of the apparatus

*Measurement cell.* The experimental set-up is shown in Figure 1. It is the same already described elsewhere,<sup>2,3</sup> so it will be only shortly described here. The measuring cell (1), with a volume of approximately  $47 \text{ cm}^3$ , was made out of a stainless steel cylinder. A stirrer (3), consisting of a stainless steel rod having a rounded end with two steel blades welded onto, was placed in the cell. The purpose of the stirrer was to prevent any premature stratification of the fluids comprising the various mixtures, while also assuring a greater homogeneity during the liquefaction and crystallization of the mixture. The stirrer inside the cell was turned by a magnet (4), which drives the plate welded onto the lower end of the rod and shaped so as to follow the bottom of the cell as

faithfully as possible. Two holes were made in the cover and a stainless steel tube was inserted through and welded to the first hole for charging the cell with gas, while the second hole was used to contain the thermometer (2). The magnet was housed in a seat made of brass, which was connected to the shaft of an electric engine (5) driving the rotation of the magnet and thus also of the stirrer inside the cell.

The cooling system globally included four parts:

1. A coil consisting of copper tube, placed inside a Dewar filled with liquid nitrogen (6), which absorbs heat from the carrier fluid (compressed air) flowing inside it;
2. a coil with the same structural features as above, wrapped around the measuring cell and removing heat from the cell by surface contact due to the cold air circulating inside it. The assembly consisting of the coil and the cell, suitably coated with neoprene, was placed inside a second Dewar (7) so as to increase its thermal isolation;
3. a double pipe heat exchanger (8): the diameter of the tubes were 6 mm for the inner tube and 16 mm for the outer tube. A flow of air at room temperature entered the exchanger's inner tube and, as it moved through the tube, it was cooled by the backflow heat exchange with the cold air leaving the coil wrapped around the measuring cell. The carrier fluid can thus be pre-cooled, enabling a considerable saving of liquid nitrogen consumption;
4. an ice trap (9) consisting of a copper base to ensure the stratification on the inside walls of the ice that forms after the liquefaction and subsequent solidification of the humidity in the carrier fluid circulating in the first coil.

A dry air supplier (10) was installed to overcome any problems relating air humidity, which would have interfered with its free flow inside the coils, especially at the low temperatures.

A mass flow control was installed upstream from the dehumidifier (11). The airflow was also measured by a rotameter (12).

An absolute pressure transducer (HBM, mod. P8A) (13) was installed in the charging tube.

*Temperature measuring systems.* To monitor the temperatures, the apparatus was equipped with one

thermoreistance put in the measuring cell. The system parameters and the efficiency of the regenerative exchanger and of the coil immersed in the liquid nitrogen were assessed using thermocouples at specific points on the copper tube. The platinum resistance thermometer used in the apparatus (100  $\Omega$ , Minco, mod. S7929) was calibrated by comparison with a 25  $\Omega$  platinum resistance thermometer (Hart Scientific, mod. 5680 SN1083).

### **Experimental procedure and uncertainties**

Given the experimental set-up, the measuring cell volume was not separated from the rest of the apparatus. So, the total volume is a sum of the cell volume and of the tube volume. Since the volume of the cell was known from the design data, we also estimated the volume of the tube used to charge it. The aim was to correct the experimental data obtained by estimating the masses of the charged fluids that did not enter the cell, but remained in the rest of the volume.

*Experimental procedure.* The bottle containing the refrigerant gas (14) was weighed on the electronic balance; then the bottle was connected to the apparatus and to the vacuum pump (15) (Vacuubrand, mod. RZ2), a vacuum was created inside the measuring cell and the charging tube as recorded on the vacuum pump gauge (Galileo, mod. OG510); then the fluid was charged by opening the valve on the gas bottle; the temperature of the cell was decreased by a flow of compressed air cooled with liquid nitrogen so as to insert the whole mass in the cell, leaving as little as possible in the charging tube; then the on/off valve was closed; the gas bottle was disconnected and weighed again to establish the actual mass charged in the cell.

The air was cooled by putting the coil inside a dewar filled with liquid nitrogen. The coil was then wrapped around the measuring cell. During the measurement procedure, the temperature of the sample inside the cell was carefully controlled to fall at uniform rate by the air flowing inside the coil. Monitoring the time dependence of temperature, a cooling curve was obtained for each sample concentration. While the change of phase occurs, the heat removed by cooling is compensated by the latent heat of the phase change, showing a temperature drop as showed in Figure 2. The arrest in

cooling during solidification allows the melting point of the material to be identified on the time-temperature curve. To give a phase diagram, the melting points can be plotted versus the composition.

*Uncertainties.* All the uncertainties were calculated using the law of error propagation, as reported elsewhere.<sup>3</sup> Here, the previously reported results will be briefly summarized.

The uncertainty in the mass of fluid charged in the measuring cell was less than  $\pm 0.008$  g for a pure fluid. The total uncertainty of the mass of sample mixture was less than  $\pm 0.01$  g. As a result, the uncertainty in density, calculated with the law of error propagation, was never greater than  $\pm 0.05$  g/dm<sup>3</sup>. The uncertainty in composition measurements was estimated to be always lower than 0.005 in mole fraction.

The uncertainty for the pressures measured for the triple points was calculated to be less than  $\pm 3$  kPa.

The total uncertainty for the thermoresistance, using the law of error propagation, was calculated to be less than  $\pm 0.023$  K.

## **Experimental results**

*Chemicals.* Carbon dioxide and nitrous oxide were supplied by Sol SpA. Their purity was checked by gas chromatography, using a thermal conductivity detector, and was found to be 99.99% for both fluids, basing all estimations on an area response. R152a was supplied by Union Carbide; its purity was found to be 99.94% on an area response.

*Pure fluids.* For carbon dioxide and nitrous oxide, the tests conducted with the stirrer switched off revealed a wider metastable phase than in the tests conducted with the stirrer turning inside the cell: this is probably due to the perturbation induced by the stirrer which reduces the time margin for the supercooling phase. Another feature common to all the experiments was that a faster cooling rate coincided with a greater supercooling effect. The cooling rate that seemed to guarantee the greatest repeatability of the results was approximately  $-0.01$  K/s, corresponding to an air flow rate of

approximately  $0.17 \text{ dm}^3/\text{s}$ . Figure 2 shows an example of a measurement taken for carbon dioxide in which there was evidence of approximately 10 K of supercooling.

For R152a, the metastable phase was not appearing during the measurements, and only a change of slope was evident in the temperature-time diagram, as witnessed by Figure 3.

Table 1 summarizes the temperatures recorded at the triple point for the pure fluids and the reference data for these fluids.<sup>4-9</sup> The comparison with the literature<sup>5</sup> data shows a very good agreement in the triple point measurements for  $\text{CO}_2$  in terms of temperature while a discrepancy of 5 kPa was found in terms of pressure. Slightly higher discrepancy, even well within the experimental uncertainty, for  $\text{N}_2\text{O}$  and R152a with literature<sup>6-9</sup> was evident for triple point temperatures.

*Results for mixtures.* Regarding the mixtures with constituents considered, there are no data on the SLE in the literature, so the present study covers new ground and the data we obtained can be used as the starting point for future studies. Measurements were taken using different concentrations of the two components, obtaining a satisfactory number of points, which were then recorded on a concentration/temperature graph ( $T$ - $x$ ).

Conducting several tests on the same sample, we noted that we obtained better, more reliable results by switching off the stirrer before reaching the triple point temperature. The turning of the stirrer helps to keep the mixture's components or sample well mixed and the homogeneity of temperature inside the cell, but once near-freezing temperatures have been reached, it probably interferes with the solidification of the mixture. We consequently decided to turn off the stirrer at least about 20-40 K (values suggested by experience) beforehand in all the subsequent tests so as to avoid losing the beneficial effect of the stirrer while also avoiding any fragmentation of the solid crystals when they began to form.

The  $T$ - $x$  measurements for the two mixtures considered ( $\text{CO}_2 + \text{R152a}$  and  $\text{N}_2\text{O} + \text{R152a}$ , respectively) are given in the figures 3 and 4. The results were also summarized in Table 2. From

the  $T$ - $x$  data it is evident that both systems form eutectics ( $x_1 = 0.09$  at  $T = 144$  K for  $\text{CO}_2 + \text{R152a}$  and  $x_1 = 0.19$  at  $T = 132$  K for  $\text{N}_2\text{O} + \text{R152a}$ ).

Since the measured vapor pressure data were not accurately measured at very low temperatures within declared precision of the used instrument (the pressure values were acquired by an absolute pressure transducer HBM, mod. P8A, and the global uncertainty of the pressure measurements was estimated to be less than  $\pm 3$  kPa)<sup>3</sup>, the vapor pressure data were not reported in the present paper.

*Rossini method corrections.* The results of the temperature data acquisitions were corrected using the Rossini method<sup>10</sup> because a constant cooling rate is not indispensable and was not guaranteed by our experimental method. This is a graphic method that considers the area contained by the tangent to the curve in the descending stretch after the temperature drop, and curve itself; then a vertical segment (a) is taken, which divides the area into two equal parts; then a second, horizontal segment (b) is obtained, from the point of intersection between the segment (a) and the tangent to the curve, up until it identifies the temperature corresponding to this new point on the axis of the ordinates ( $T_m$ ). This graphic method is illustrated in Figure 2. The entity of the corrections takes into account the fact that the fluid is still in a liquid state during the metastable state (supercooling) that precedes proper solidification. In this phase, the temperature is distinctly lower than the one characterizing the instant when crystallization begins, its amplitude depending mainly on the rate at which the temperature is lowered. The resulting corrections were nonetheless always very limited, of the order of a few tenths of a Kelvin in the majority of cases, and always well below 1 K.

### **Interpretation of the results**

Most organic systems form eutectics: in this case, the course of the *liquidus* is well described by the Schröder equation, known since the end of the 19<sup>th</sup> century.<sup>11</sup> The SLE depend both on the crystals formed in solution and on the properties of the liquid phase. The exact course of the *liquidus* for ideal mixtures (i.e. showing a small deviation from Raoult's law) depends mainly on the property of



the solute (CO<sub>2</sub> and N<sub>2</sub>O in our case) and, in the case of non-ideal systems, on the property of the liquid phase.

As both systems formed eutectics, the solubility of the solid solute in the solvent (here, R152a) can be described by the Schröder equation; which disregarding any difference between the heat capacity of the subcooled liquid solute and solid solute takes the following form:

$$\ln \gamma_2 x_2 = -\frac{\Delta h_m}{RT} \left( 1 - \frac{T}{T_m} \right) \quad (1)$$

where the subscript 2 denotes the solute and the subscript m denotes property at melting point.

Assuming as a first approximation that the solute's activity coefficient,  $\gamma_2=1$ , we can write:

$$\ln x_2 = -\frac{\Delta h_m}{RT} \left( 1 - \frac{T}{T_m} \right) \quad (2)$$

This simplification leads to the consideration that the solubility of the solid solute is independent of the solvent as far as the assumptions hold. The enthalpies at melting point ( $\Delta h_m$ ) were assumed to be 9020 J·mol<sup>-1</sup>,<sup>12</sup> 6540 J·mol<sup>-1</sup>,<sup>12</sup> and 1566 J·mol<sup>-1</sup>,<sup>9</sup> for CO<sub>2</sub>, N<sub>2</sub>O and R152a, respectively.

The course of the liquidus calculated with the Schröder equation is included in Figures 3 and 4. Both systems well followed the Schröder equation. For the CO<sub>2</sub> + R152a system a good agreement with the equation prediction was evident. For the N<sub>2</sub>O + R152a, a general agreement with the Schröder equation was evident.

## Conclusion

In this paper, the SLE behavior of CO<sub>2</sub> + R152a and N<sub>2</sub>O + R152a was measured down to temperatures of 132 K. The apparatus enabled us to record temperature and composition data. The triple points of the pure fluids contained in the mixture were measured to check the reliability of the new apparatus, revealing a good consistency with the literature. The CO<sub>2</sub> + R152a and N<sub>2</sub>O + R152a systems showed the presence of an eutectic ( $x_1 = 0.09$  at  $T = 144$  K for CO<sub>2</sub> + R152a and  $x_1 = 0.19$  at  $T = 132$  K for N<sub>2</sub>O + R152a) and of a good agreement with Schröder equation prediction.

## References

1. Di Nicola, G.; Polonara, F.; Santori, G.; and Stryjek. R. Isochoric  $PVT_x$  Measurements for Carbon Dioxide + 1,1-difluoroethane Binary Systems. *J. Chem. Eng. Data* **2007**, 52, 1258-1261.
2. Di Nicola, G.; Giuliani, G.; Polonara, F.; and Stryjek. R. Solid-liquid equilibria in the  $\text{CO}_2$  +  $\text{N}_2\text{O}$ ,  $\text{CO}_2$  + R32, and  $\text{N}_2\text{O}$  + R32 systems. *Fluid Phase Equilib.* **2007**, 256, 86-92.
3. Di Nicola, G.; Giuliani, G.; Polonara, F.; and Stryjek. R. Solid-liquid equilibria for the  $\text{CO}_2$  + R125, and  $\text{N}_2\text{O}$  + R125 systems: a new apparatus. *J. Chem. Eng. Data* **2006**, 51, 2209-2214.
4. Marsh, K. N. Recommended Reference Materials for the Realization of Physicochemical Properties, Blackwell Sci. Pub., Oxford, 1987.
5. Angus, S.; Armstrong, B.; and de Reuck, K. M. International Thermodynamic Tables of the Fluid State - 3 Carbon Dioxide, Pergamon, New York, 1976.
6. Fonseca, I. M. A.; Lobo, L. Q. Thermodynamics of liquid mixtures of xenon and methyl fluoride. *Fluid Phase Equilib.* **1989**, 47, 249-263.
7. Calado, J. C. G.; Rebelo, L. P. N.; Streett, W. B.; and Zollweg, J. A. Thermodynamics of liquid (dimethylether + xenon) *J. Chem. Thermodyn.* **1986**, 18, 931-938.
8. Blanke, W; Weiss, R. Isochoric (p,v,T) measurements on  $\text{C}_2\text{H}_4\text{F}_2$  (R152a) in the liquid state from the triple point to 450 K and at pressures up to 30 MPa. *Fluid Phase Equilib.* **1992**, 80, 179-190.
9. Magee J.W. Molar heat capacity at constant volume of 1,1-difluoroethane (R152a) and 1,1,1-trifluoroethane (R143a) from the triple-point temperature to 345 K at pressures to 35 MPa. *Int. J. Thermophys.* **1998**, 19, 1397-1411.
10. Mair, B.J.; Glasgow, J.A.R.; and Rossini, F.D. Determination of the freezing points and amounts of impurity in hydrocarbons from freezing and melting curves. *J. Res. Nat. Bur. Standards* **1941**, 26, 591-620.

11. Schröder, I. Über die Abhängigkeit der Löslichkeit eines festen Körpers von seiner Schmelztemperatur. *Z. Phys. Chem.* **1893**, 11, 449-465.
12. Lide, D. R.; and Kehiaian, H. V. *CRC Handbook of Thermophysical and Thermochemical Data*. CRC press, Inc. 1994.

## Figure captions

Figure 1. Schematic illustration of the apparatus.

Notation:

1. Measurement cell
2. Platinum resistance thermometer
3. Stirrer
4. Magnet
5. Electric engine
6. Dewar with liquid nitrogen
7. Dewar containing the measurement cell
8. Double pipe heat exchanger
9. Ice trap
10. Dry air supplier
11. Mass flow controller
12. Rotameter
13. Pressure trasducer
14. Charging bottle
15. Vacuum pump system

Figure 2. Acquisition of the CO<sub>2</sub> triple point temperature measurements and Rossini method illustration.

Figure 3. Acquisition of the R152a triple point temperature measurements.

Figure 4. SLE for the CO<sub>2</sub> + R152a system. Black symbols denote the experimental points while the lines denote the Schröder eq.

Figure 5. SLE for the N<sub>2</sub>O + R152a system. Black symbols denote the experimental points while the lines denote the Schröder eq.

Table 1. Average Temperature and Pressure Triple Point Measurements for the Pure Fluids

Fluid	$T/\text{K}$	$P/\text{kPa}$	$T_{lit}/\text{K}$	$P_{lit}/\text{kPa}$
CO <sub>2</sub>	216.56	514	216.59 <sup>4,5</sup>	519 <sup>5</sup>
N <sub>2</sub> O	181.99	92	182.34 <sup>6,7</sup>	90 <sup>6,7</sup>
R152a	154.30	-	154.56 <sup>8,9</sup>	0.065 <sup>9</sup>

Table 2.  $T$ - $x$  Measurements for the  $\text{CO}_2 + \text{R152a}$  and  $\text{N}_2\text{O} + \text{R152a}$  Binary Systems.

$\text{CO}_2$ (1) + R152a (2)		$\text{N}_2\text{O}$ (1) + R152a (2)	
$x_1$	$T / \text{K}$	$x_1$	$T / \text{K}$
0.000	153.20	0.000	153.20
0.030	152.20	0.039	150.34
0.055	147.48	0.081	143.95
0.064	146.37	0.133	138.58
0.094	148.65	0.186	132.30
0.150	158.15	0.223	135.05
0.185	161.54	0.289	140.85
0.315	176.52	0.436	151.87
0.457	187.51	0.489	155.24
0.559	193.95	0.632	164.08
0.668	199.50	0.719	169.51
0.755	205.77	0.819	174.38
0.769	205.38	0.879	177.87
0.860	209.38	1.000	181.90
0.901	211.27		
1.000	216.52		

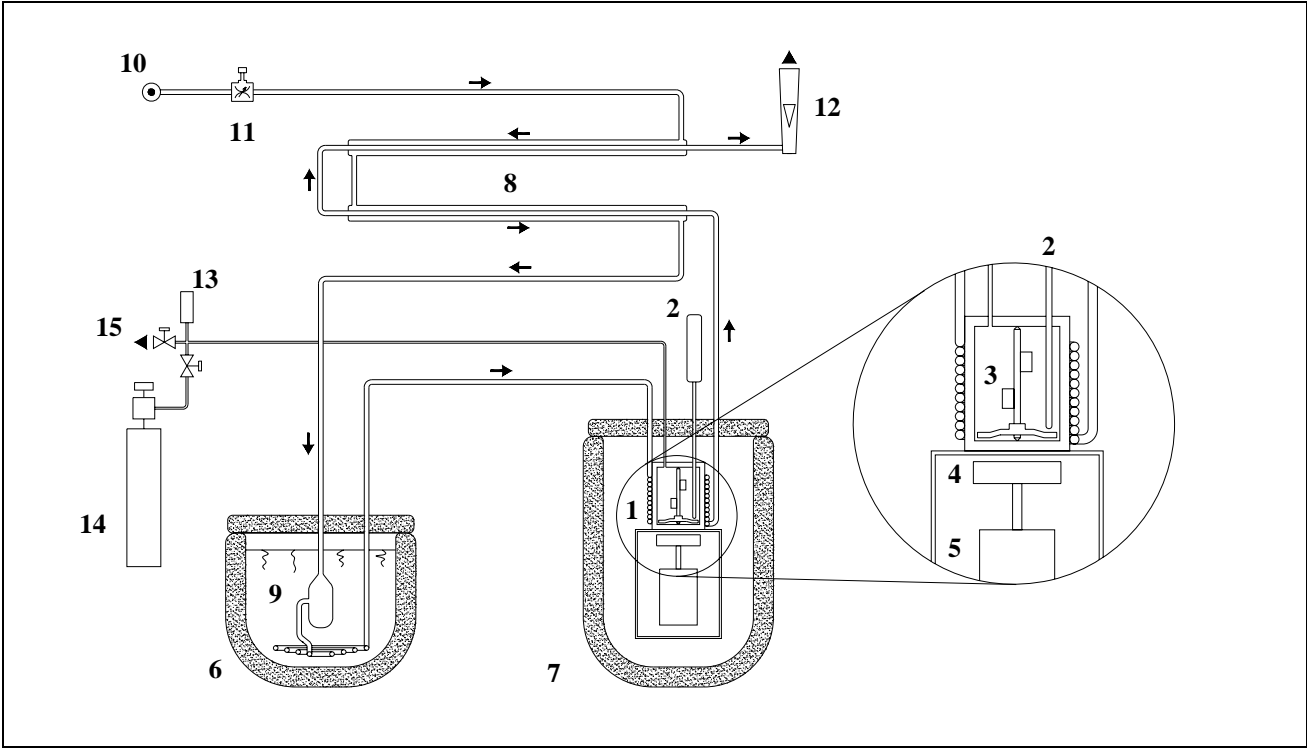


Figure 1

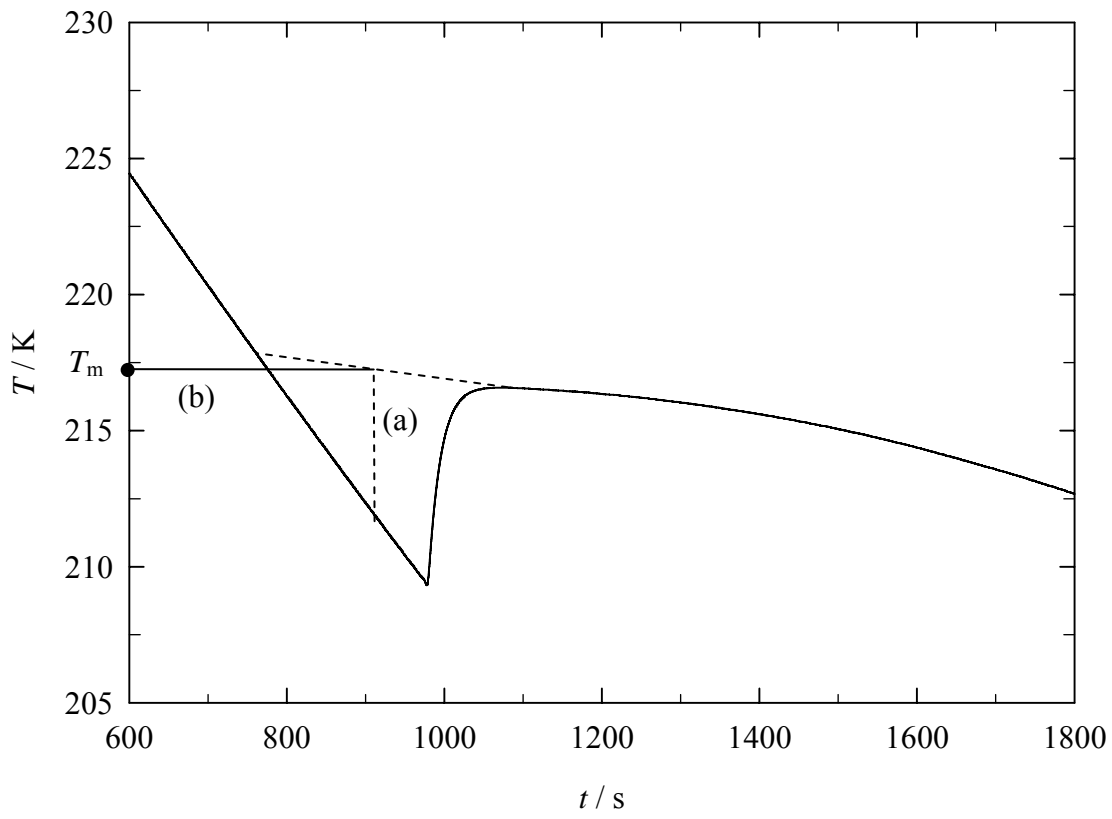


Figure 2.



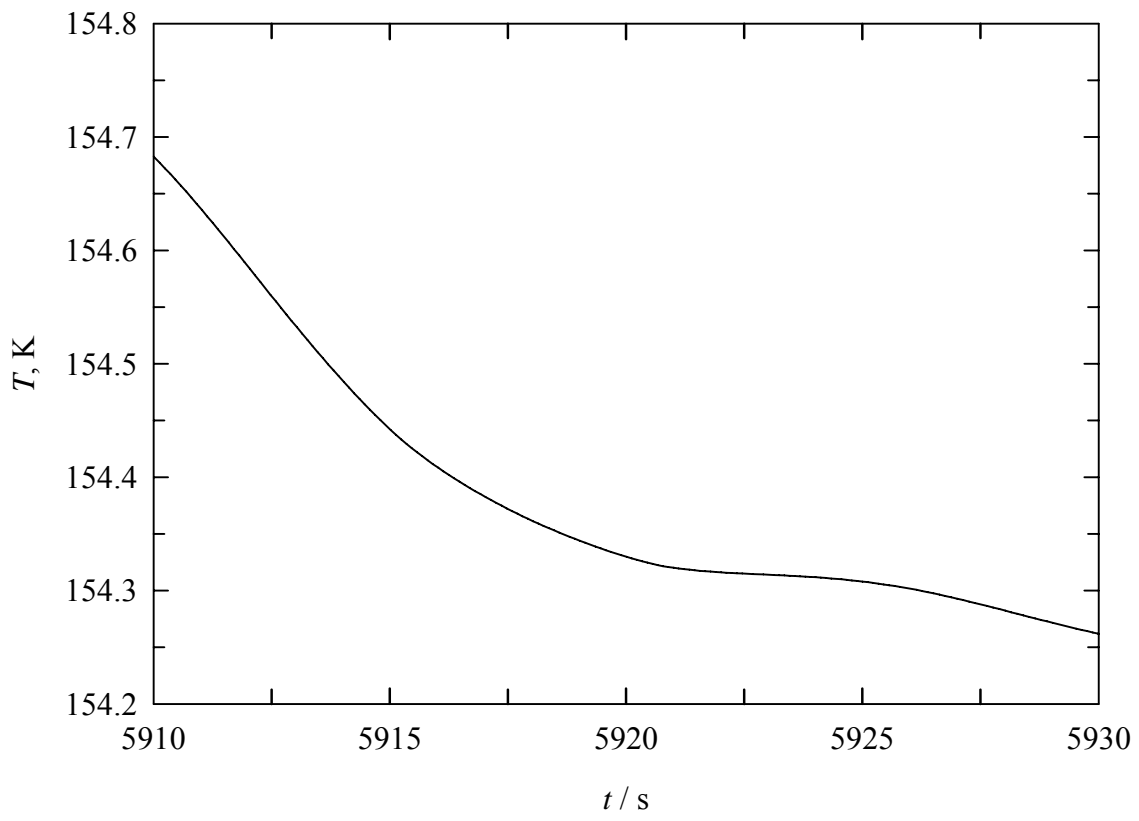


Figure 3.

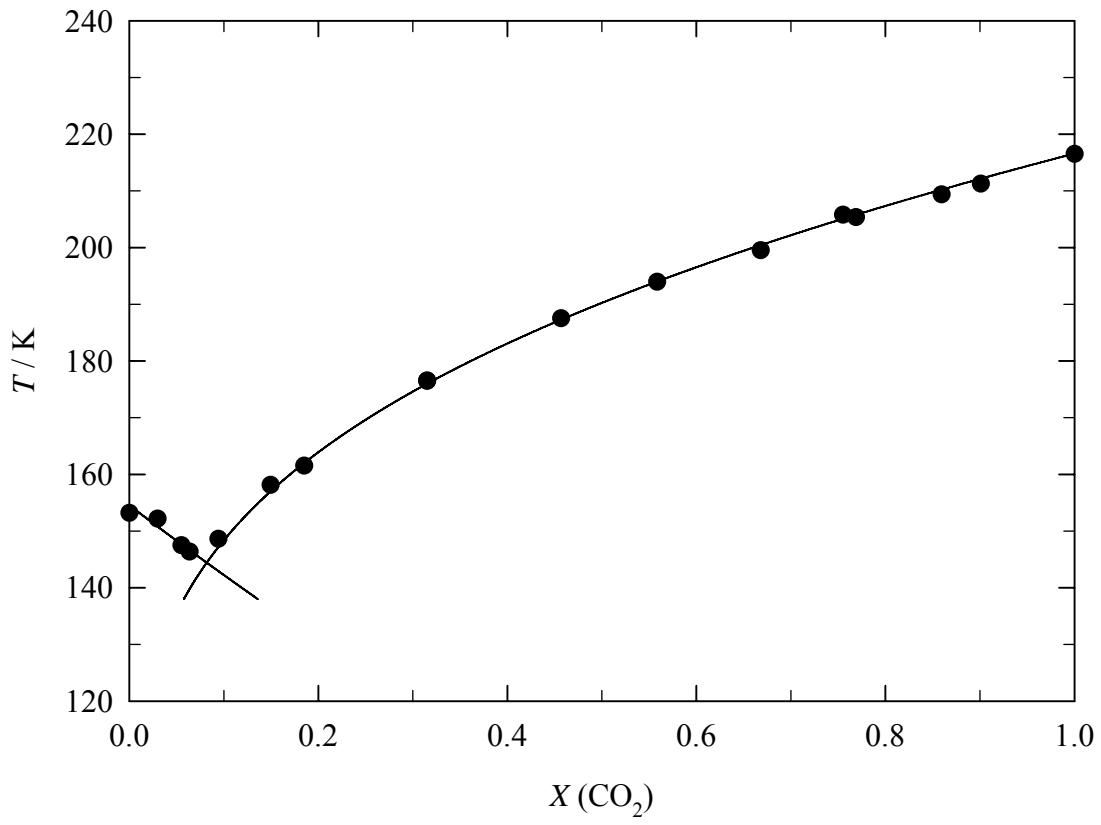


Figure 4.

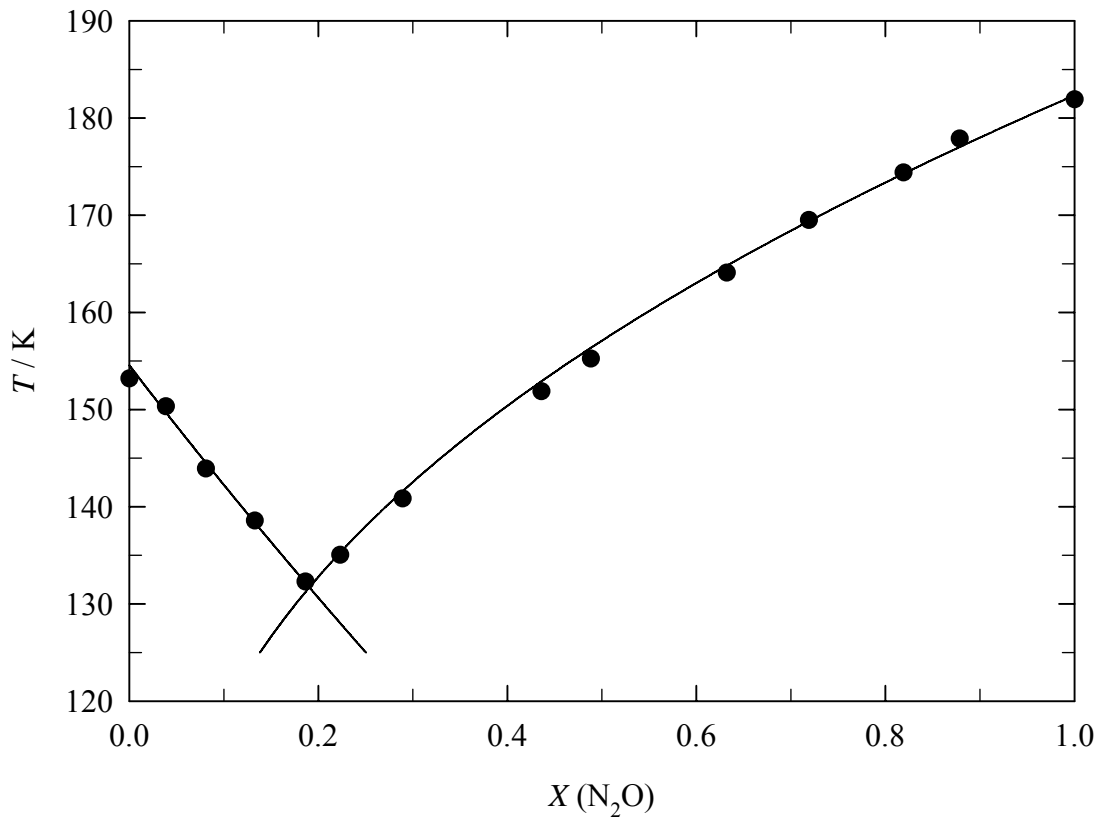


Figure 5.